ISSN 1027-5495. Functional Materials, 27, No.4 (2020), p. 710-715.
doi:https://doi.org/10.15407/fm27.04.710

Structural and phase composition features of titanium and chromium nitride coatings obtained by ion-plasma deposition

***D.B.Hlushkova*[1], *A.I.Voronkov*[1], *N.E.Kalinina*[2], *V.T.Kalinin*[3], *L.H.Polonskyi*[4], *A.I.Stepaniuk*[1]**

[1]Kharkiv National Automobile and Highway University, 25 Y.Mudrogo Str., 61002 Kharkiv, Ukraine
[2]O.Honchar Dnipro National University, 72 Gagarin Ave., 49010 Dnipro, Ukraine
[3]National Metallurgical Academy of Ukraine, 4 Gagarin Ave., 49600 Dnipro, Ukraine
[4]Zhytomyr Polytechnic State University, 103 Chudnivska Str., 10005 Zhytomyr, Ukraine

Received July 12, 2020

Phase composition, texture, and stress state in coatings based on Ti–N, Cr–N, and Ti–Cr–N systems obtained by ion-plasma deposition method are studied using an X-ray difractometry (by structural analysis) Texture and high compressive stresses up to ~ 3 GPa are revealed in all observed phases (TiN, Cr_2N). Factors affecting the residual-stress level are discussed, and the model of stress-state formation is proposed.

Keywords: titanium nitrides, chromium nitrides, X-ray diffractometry, coatings, residual stresses, texture, phase composition.

Особливості структури і фазового складу покриттів нітридів титану та хрому, які отримують методом іоно-плазмового осадження. *Д.Б.Глушкова, А.І.Воронков, Н.Є.Калініна, В.Т.Калінін, Л.Г.Полонський, А.І.Степанюк*

Методом аналізу структури досліджено фазовий склад, текстуру і напружений стан е покриттях на основі систем Ti–N, Cr–N, Ti–Cr–N, отриманих методом плазмового осадження. У всіх виявлених фазах (TiN, Cr_2N) виявлено текстуру і великі стискаючі напруження, що досягають значення ~ 3 ГПа. Обговорено чинники, що впливають на рівень залишкових напружень, запропоновано модель формування напруженого стану.

Методом анализа структуры исследованы фазовый состав, текстура и напряженное состояние в покрытиях на основе систем Ti–N, Cr–N, Ti–Cr–N, полученных методом плазменного осаждения. В выявленных фазах (TiN, Cr_2N) обнаружена текстура и значительные сжимающие напряжения, достигающие ~ 3 ГПа. Обсуждены факторы, влияющие на уровень остаточных напряжений, предложена модель формирования напряженного состояния в покрытиях на основе нитрида титана и хрома.

1. Introduction

It is known that one of the ways to increase the material wear resistance is to modify its surface using methods of ion-plasma deposition of strengthening coatings [1–3]. Coatings based on transition metal nitrides are promising coatings for die tools, as well as for friction units [3]. However, there are currently no studies of the stress state for

coatings of complex chemical composition formed under non-equilibrium conditions and associated with self-organization of dissipative structures. This complicates the optimization of the technology for obtaining coatings with the specified structure and properties [4]. This work is aimed to study the structure, phase composition of applied coatings in order to construct the model for the ion-plasma coating formation, taking into account the parameters of their production.

2. Experimental

Coatings of titanium and chromium nitrides with a thickness of 1.5–3.5 μm were applied by vacuum-arc method using the Bulat-ZT plant on steel 20 substrates. The method includes two main stages [2]. At 1st stage, the substrate surface was cleaned and activated by ion bombardment with the deposited material at a displacement potential of 1,400 V. The radiation heating of the substrate, depending on the substrate material, did not exceed 500°C. At the 2nd stage, the coating was deposited.

The coatings were produced by sputtering of high-purity titanium and chromium based cathodes in a purified nitrogen medium at the pressure maintained at 0.3 Pa. The bias potential and ionic current were 200 V and 1.5 A for titanium deposition and 150 V and 0.8 A for chromium deposition. The thickness of the coatings was changed by increasing the deposition time from 5 to 15 min when the substrate is rotated at a speed of 8 min^{-1}. The coating of the Ti–Cr–N system was obtained by simultaneous sputtering of titanium and chromium cathodes at the bias potential of 150 V.

The objects of X-ray diffraction studies were the "film on a substrate" systems. Studies were performed in the radiation of a copper anode with monochromatization in a diffracted beam. To identify the structure and texture, measurements were made in the range of 2ψ angles from 20° to 150°. Determination of residual deformations in coatings was performed using the $\sin^2\psi$ method by precision measurement of interplane distances during multiple inclined surveys. As the angle of inclination increases, the thickness of the informative layer naturally decreases [4].

3. Results and discussion

3.1. Residual stresses in TiN coatings

Figure 1 shows the displacement of the diffraction lines of titanium nitride Ti–N at different angles ψ, which indicates the presence of internal stresses.

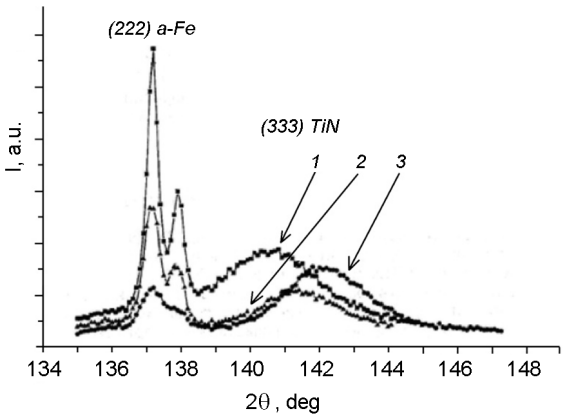

Fig. 1. Changing the type of the diffractogram section using inclined surveys of the sample with TiN coating of 1.9 μm thick: *1* — ψ = 0°, *2* — ψ = 30°, *3* — ψ = 50°.

Analysis of diffractograms of Ti–N coatings on the substrate showed that they reveal lines corresponding to the TiN phase (NaCl structural type) and lines of the α-phase (ferrite) corresponding to the reflection from the substrate. Therewith, reflections from the α-phase are present at all ψ values. It follows that the entire thickness of the coating is involved in the formation of the diffraction pattern.

TiN type diffraction lines (*hhh*) are much more intense in reflection compared to tabular data, which indicates TiN texturing. An axial-type texture with the axis (111) perpendicular to the substrate plane and the diffusion angle of the texture $\Delta p \geq 15°$ is detected.

The stress state was analyzed using the (333) TiN and (222) α-phase reflections (Fig. 1). As the angle ψ increases from 0 to 50°, the intensity of the (333) TiN line increases, and the (222) α-phase line weakens. In addition, the (333) TiN line s noticeably shifted towards large angles, while the position of the (222) α-Fe phase line practically does not change. The (222) α-Fe phase line present on the diffractogram is a reflection from the substrate as a result of a thin coating. The positions *1, 2, 3* correspond to the registration of the same (333) Ti–N line obtained at different angles of inclination of the sample with TiN coating with the thickness of 1.9 μm: *1* — ψ = 0°, *2* — ψ = 30°, *3* — ψ = 50°. It is means that compressive stresses act in the film plane, and stresses are not detected radiographically in the substrate.

According to the figure, the positions of the diffraction lines were determined and the lattice period was found in accordance with the formulas.

The graphs of the diffraction profiles $\alpha_\psi - \sin^2\psi$ based on the results of processing are shown in Fig. 2. It should be noted that the graphs are symmetric with respect to the slope of the sample towards $\psi > 0$ and $\psi < 0$. Experimental points are not described by a strictly linear relationship. The deviation from the linear relationship (curve *1*) exceeds the error of lattice period determination, which is $\pm 3 \cdot 10^{-4}$ Å. However, by approximating the graphs with straight lines, it is possible to estimate the average deformation over the coating thickness ε in accordance with the relations:

$$a_\psi = \frac{a_0(1+\upsilon)}{E}\sigma_\psi \sin^2\psi + a_{\perp\psi}, \qquad (1)$$

$$\varepsilon = \frac{a_{\psi=90} - a_{\psi=0}}{a_0} = \frac{a_\parallel - a_\perp}{a_0}, \qquad (2)$$

where $\alpha_\perp$ is value of the lattice period in the direction normal to the reflecting planes ($\psi = 0°$); $\alpha_\parallel$ is the value of the lattice period in the film plane ($\psi = 90°$); a_0 is the value of the lattice period in non-tensioned condition; σ_φ is normal stress components in the plane of the coating; υ is Poisson ratio; E is Young's modulus.

The average ε deformation values are –0.82 % for the sample with a thickness of 1.9 μm and –0.98 % for a sample with a thickness of 3.2 μm.

Line 2 on the graph describes compressive stresses that are uniform throughout the entire reflecting layer. To calculate macrostresses, it is necessary to know υ Poisson's ratio and E modulus of normal elasticity. The data on these parameters for TiN are contradictory in the literature. For values $\upsilon = 0.23$ and $E = 429$ GPa [5], the following values of macrostresses in the TiN phase were obtained: $\sigma = -3.1$ GPa for a coating with the thickness of 1.9 μm; $\sigma = -3.4$ GPa for a coating with a thickness of 3.2 μm.

The lattice period α_0 can be determined from $\sin^2\psi$ — graphs under the assumption of an isotropic symmetric plane-stressed state. It is determined at the ψ_0 value corresponding to the undeformed section of the deformation ellipsoid:

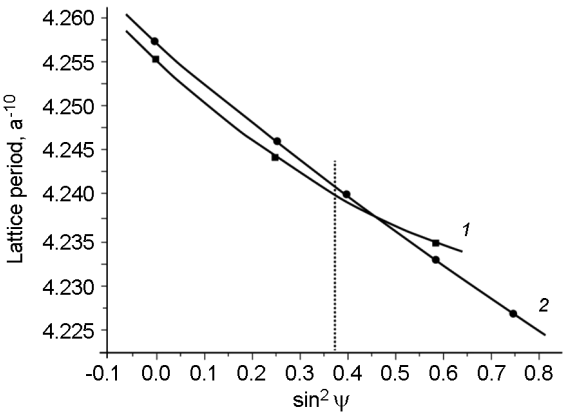

Fig. 2. Graph of the dependence of the lattice period on $\sin^2\psi$ for (333) TiN: *1* — coating thickness 1.9 μm, *2* — coating thickness 3.2 μm.

$$\sin^2\psi_0 = \frac{2\upsilon}{1+\upsilon}. \qquad (3)$$

As can be seen from Fig. 2, the value of α_0 in coatings of different thicknesses is almost the same for samples obtained under equivalent conditions, and is equal to $\alpha_0 = 4.2415$ Å. The value of α_0 differs from the value of the TiN lattice period of stoichiometric composition equal to 4.243 [6], but it coincides with the data of [7]. TiN, as an implementation phase, is characterized by a wide area of homogeneity. Estimates show that the value of α_0 obtained in this work indicates that the deviation from the stoichiometric composition in TiN coatings does not exceed ±10 % of atm. nitrogen.

3.2. Research of Cr–N coatings

Diffractograms of Cr–N coatings show intense Cr_2N phase lines with the hexagonal lattice, weak chromium lines with BCC lattice, and α-phase lines (from the substrate). Significant intensity of the Cr_2N (h00) type phase lines indicates the presence of an axial type texture with (h00) planes located mainly parallel to the surface of the coating. The diffusion angle of the texture is $\Delta\rho \sim 20°$.

The presence of this texture is confirmed by the results of measurements in the sliding geometry, when these planes are approximately perpendicular to the surface plane and come out of the reflecting position.

As a result of, it was found that a thin chromium sublayer is initially formed on the steel substrate, and a Cr_2N coating is formed on it.

In order to measure macro-deformations and determine the lattice periods in the

Cr_2N phase, (411) and (223) reflections located in the range of diffraction angles 2ψ 110–125° were selected. For these reflections, the $d_\psi - \sin^2\psi$ dependences are constructed, which are shown in Fig. 3. Figure 3 shows that all values of Cr_2N interplane distances in a thinner sample are higher. $Sin^2\psi$ graphs for the diffraction line (223) have a similar form.

The average level of compressive macrodeformations in the samples ranges from –1.3 % to –1.0 %. In a thin surface layer, the value of residual deformations based on the results of surveys in the sliding geometry coincides with the given values. The periods of the Cr_2N crystal lattice calculated from the values of the interplane distances d (411) and d (223) in the undeformed section of a sample with a thickness of 3.0 μm are $a_0 = 2.776$ Å and $c_0 = 4.447$ Å. When evaluating, it was assumed that $v = 0.23$, as for CrN [10]. The lattice period values for a thin sample are higher: $a_0 = 2.783$ Å and $a_0 = 4.471$ Å. All the obtained values of the lattice periods are within the region of homogeneity of the Cr_2N phase [8, 9].

A complex phase composition is detected in the Ti–Cr–N sample with the thickness of 1.6 μm within the reflecting layer. The diffractogram contains lines belonging to the TiN and Cr_2N phases, lines of the chromium layer, and substrates. Analysis of the intensity ratio of diffraction lines indicates that the Ti–Cr–N coating shows a weaker texture than in single-phase films.

The lines of the detected phases, as in the case of single-phase films, are shifted towards smaller angles, which gave reason to assume the presence of compressive residual stresses in the coating. Estimation of macrodeformations and stresses in titanium nitride was performed using sin2ψ method along the line (422) with the largest angle 2θ of the detected reflections.

The phase composition of the studied samples is characterized by the presence of TiN or Cr_2N phases. Ti_2N and CrN phases are not detected. This can be explained as follows. According to the phase equilibrium diagrams of Ti–N and Cr–N systems [12, 13], the Cr_2N and TiN phases are formed by the peritectic reaction. In quasi-equilibrium conditions of vacuum condensation by the "vapor-crystal" mechanism [10], they can be formed as result of a gas-peritectic reaction near the substrate surface. The CrN and Ti_2N phases can be obtained at appropriate temperatures and deposition times by

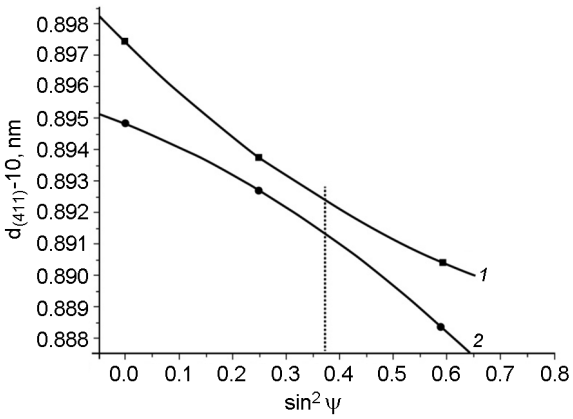

Fig. 3. $d_\psi - \sin^2\psi$ graph for (411) Cr_2N: *1* is coating thickness 1.3 μm, *2* is coating thickness 3.0 μm.

peritectoid reactions in the solid state involving previously formed solid nitrides Cr_2N and TiN. Under the coating conditions used, the formation of CrN and Ti_2N is suppressed by the kinetic factor.

Under simultaneous evaporation of titanium and chromium in the nitrogen atmosphere, the main phase in the coating is TiN. Titanium interacts with nitrogen because of its higher affinity for nitrogen than chromium. Thus, the free energy of the formation reaction TiN ($-\Delta G$) is 2.6 times higher than that of Cr_2N, and the reaction rate constant is about 1.5 times higher [11].

A feature of the structural state of the coatings studied with X-rays is the presence of significant compressive stresses and textures, which are naturally associated with deposition modes. Similar results observed earlier in the study of films deposited from streams by various physical methods were widely described by the authors [6–8]. At the same time, the influence of individual factors in the coating structure formation, such as "atomic forging" (pinning) [3, 4], "compaction" [12], "collision of crystallites" [13], was analyzed. However, to date, there is no reasonable explanation for the formation of abnormally high deformations, which often exceed 1 %, which is significantly higher than the usual elastic limit of samples having metallurgical origin.

The data obtained in this work on the phase composition, structure, substructure, texture, and stress state of coatings of various thicknesses give grounds to consider the process of film formation from the point of view of the structure evolution and its self-organization in the framework of an irreversible multiparametric thermodynamic

process. Main idea of this approach is that if the "growing film on a substrate" system experiences a range of energy effects during the coating formation, then it develops a number of energy dissipation directions and responses of the system itself, such that the total Gibbs energy of the "film-substrate" system is minimal. In this case, the "film" can be heterophase and inhomogeneous initially or become so during the development of the system. In a multi-level structure system (macro -, micro- and submicrostructural levels), the dissipation of the supplied and locally stored energy must also occur multilevel and not uniformly in volume. From the point of view of elasticity theory, this causes the formation of residual deformations localized at the level of macro -, micro - and submicrostructure. However, the operator, value and distribution of stresses must be related to the structural and textured state.

Microstresses in melts are balanced within individual grains, but have a common orientation of the main directions in each grain, due, for example, to the oriented influence of the long-range part of the displacement fields around defects.

During the formation of coatings from low-energy particle fluxes, the formation of radiation defects such as dislocation insertion loops was observed [14]. The loops should be located in tightly packed planes, the orientation of which in relation to the sample surface is associated with the predominant orientation of the crystallites. Defects of this type lead to displacement of the diffraction lines [15]. Thus, the stress values determined from the offset of the diffraction lines from the $\sin^2\psi$ graphs are the sum of the first and second kind of stresses averaged over the reflecting volume:

$$\sigma_{res}^{\sin^2\psi} = \sigma_1 + \sigma_{\parallel}^{or}, \qquad (4)$$

The differences in the stress level in the X-ray data and the deflection of the substrate shown in [16] can be explained by the action of the sum of stresses, not only σ_1, measured from the deflection. The deformation reaches the maximum limit and has the same sign, and the calculated stresses will be abnormally high.

In turn, the residual macro-stresses detected in coatings can be represented as the sum of thermal stresses σ_1^{therm} caused by the difference in the coefficients of thermal expansion of the film and the substrate, and structurally σ_1^{str}, conditioned by an inhomogeneous change in the specific volume. This change may occur as a result of crystallization of the amorphous phase, atomic pinning, or annealing of structural defects. Thus:

$$\sigma_{res}^{\sin^2\psi} = \sigma_1^{therm} + \sigma_1^{str} + \sigma_{\parallel}^{or}, \qquad (5)$$

When estimating the residual stresses of thermal origin in TiN films deposited on steel substrates at a temperature of ≤ 500°C, the values of compressive stresses not exceeding 1 GPa were obtained, which is significantly lower than those measured in this paper, $\sigma_{res}^{\sin^2\psi} = 3$ GPa. It is obvious that structural stresses σ_1^{str} caused by structural changes make a decisive contribution to the value of the measured residual stresses in coatings.

As can be seen from Figs. 2–3, in contrast to the classical $\sin^2\psi$ method, the nonlinear nature of $\sin^2\psi$ graphs is observed. The deviation from the linear relationship, as noted above, significantly exceeds the measurement error. The linear dependence is observed only for the TiN sample with a thickness of 3.2 μm (line 2 in Fig. 2), which indicates the uniformity of stresses and composition in the depth of the informative layer. As is known, the curvature of $\sin^2\psi$ graphs can be caused by a number of reasons: the slope of the main stress axes to the sample surface, the inhomogeneity of the stress level or composition in the film depth, and the influence of the sample texture. A comprehensive analysis of the experimental results shows that in this case, the nonlinear nature of $\sin^2\psi$ graphs is primarily due to the inhomogeneous thickness of the stress state.

A different type of dependencies is possible if the contribution of σ_1 and $\sigma_{\parallel}^{or}$ to σ_{res} varies depending on the thickness of the coating, its structural state, and the level of sophistication of the texture. Thus, the increase in the thickness of the TiN coating from 1.9 to 3.2 μm, accompanied by the 25 % decrease in the diffusion angle of the texture, causes an increase in the total σ_{res} and the increase in the convexity of the curves. In this case, the density of dislocations in the walls estimated from the broadening of diffraction lines with multiple indices increases from $9{\cdot}10^{10}$ to $25{\cdot}10^{10}$ cm^{-2}, and the density of randomly distributed dislocations decreases from $2.8{\cdot}10^{12}$ to

$1.6 \cdot 10^{12}$ cm^{-2}. This is probably due to radiation annealing of defects in the structure formed at the initial stages of coating generation. The accumulation of secondary defects in textured films, such as dislocation loops of small diameter that creates long-range distortion fields [16], should lead to the formation of $\sigma_{\parallel}^{gr}$.

4. Conclusions

Based on the results of structure and stress state studies, a model for the formation of ion-plasma condensates is constructed, taking into account specific deposition parameters and indirect data. The model is based on the assumption that the structure of layers formed at the initial stages of coating generation develops during deposition more significantly than under thermal deposition conditions.

It is established that stresses formed as a result of compaction (compression) and crystallization (stretching) are balanced between the coating and substrate and are σ_1 stresses of the first genus. The texture that is observed after crystallization is explained by the fact that the generation of crystallographically oriented grains is energetically more favorable than the generation of a highly dispersed polycrystal with a chaotic orientation of crystallites. Crystallization and texture formation in coatings partially remove residual macro stresses, but not completely, since the upper layers of the coating are continuously compacted as a result of bombardment. When the coating thickness is more than 1.5–2.0 μm, the inner layers of the film experience radiation-stimulated annealing.

Further growth of the coating can lead to a change in the contribution of these components to the overall level of residual stresses, which should be manifested in a change in the form of the $\sin 2\psi$ graph and the ratio between the deformation in the film plane and normal to it.

It is established that the development of the film structure, grain substructure and their preferred orientation, as well as the stress state are interrelated and are determined by specific technological parameters of coating application.

References

1. L.I.Pogadaev, *Probl. Mechan.Engin. Machine Reliability*, **3**, 29 (2003).
2. L.I.Tushinsky, Theory and Technology of Strengthening of Metal Alloys, Novosibirsk, Nauka (1990) [in Russian].
3. C.B.Carter, D.B.Williams. Transmission Electron Microscopy: Diffraction, Imaging, and Spectrometry, Springer, IP (2016).
4. M.Lee, X-Ray Diffraction for Materials Research: From Fundamentals to Applications, CRC Press, Hardback (2016).
5. D.B.Hlushkova, O.D.Hrinchenko, L.L.Kostina, A.P.Cholodov, *Probl. Atom. Sci. Tehn.*, **113**, 181 (2018).
6. Materials Science of Thin Films, 2nd Ed. by M.Ohrig, Academic Press (2001).
7. V.V.Kudinov, Plasma Coatings, Nauka, Moscow (2007) [in Russian].
8. A.P.Shpak, Yu.A. Kunitskii, Z.A.Samoilenko, Self-organization of Structure in Materials of Different Nature, Akademperiodika, Kyiv (2002).
9. D.S.Krikun, in: Proc. Intern. Res.-to-Practice Conf. Students, Post-Graduate and Postdoctoral Researchers "Youth and Scientific-and-Technological Advance", Kyiv (2013), p.38.
10. J.M.ZuoJohn, C.H.Spence, Advanced Transmission Electron Microscopy. Springer, NY (2017).
11. L.I.Mirkin, Structural Control of Engineering Materials: Handbook, Mashinostroenie, Moscow (1999) [in Russian].
12. J.I.Goldstein, D.E.Newbury, J.R.Michael et al., Scanning Electron Microscopy and X-Ray Microanalysis, Springer, NY (2017).
13. N.E.Kalinina, D.B.Hlushkova, O.D.Hrinchenko et al., *Probl. Atom. Sci. Tehn.*, **120**, 151 (2019).
14. D.Su, Advanced Electron Microscopy Characterization of Nanomaterials for Catalysis, v.2 (2017), p.70..
15. M.A.Krivoglaz, Theory of X-ray Scattering and Thermal Neutrons by Real Crystals, Nauka, Moscow (2000) [in Russian].
16. D.B.Hlushkova, Y.V.Ryzhkov, L.L.Kostina, S.V.Demchenko, *Probl. Atom. Sci. Tehn.*, **113**, 208 (2018).